HOKKAIDO UNIVERSITY

Title	Quantification of Large Deformation with Punching in Dual Phase Steel and Change of its Microstructure : Part II: Local Strain Mapping of Dual Phase Steel by a Combination Technique of Electron Backscatter Diffraction and Digital Image Correlation Methods
Author(s)	Nakada, Nobuo; Ikeda, Ken-ichi; Shuto, Hiroshi; Yokoi, Tatsuo; Tsuchiyama, Toshihiro; Hata, Satoshi; Nakashima, Hideharu; Takaki, Setsuo
Citation	ISIJ International, 56(11), 2077-2083 https://doi.org/10.2355/isijinternational.ISIJINT-2016-310
Issue Date	2016-11-15
Doc URL	http://hdl.handle.net/2115/75454
Rights	著作権は日本鉄鋼協会にある
Type	article
File Information	ISIJ Int. 56(11)_ 2077-2083 (2016).pdf

Instructions for use

Hokkaido University Collection of Scholarly and Academic Papers : HUSCAP

ISIJ International, Vol. 56 (2016), No. 11, pp. 2077–2083

Quantification of Large Deformation with Punching in Dual Phase Steel and Change of its Microstructure –Part II: Local Strain Mapping of Dual Phase Steel by a Combination Technique of Electron Backscatter Diffraction and Digital Image Correlation Methods

Nobuo NAKADA,[1)]* Ken-ichi IKEDA,[2)] Hiroshi SHUTO,[3)] Tatsuo YOKOI,[3)] Toshihiro TSUCHIYAMA,[4,5)] Satoshi HATA,[6)] Hideharu NAKASHIMA[6)] and Setsuo TAKAKI[4,5)]

1) Department of Materials Science and Engineering, School of Materials and Chemical Technology, Tokyo Institute of Technology, 4259 Nagatsuta-cho, Midori-ku, Yokohama, Kanagawa, 226-8503 Japan. 2) Division of Materials Science and Engineering, Faculty of Engineering, Hokkaido University, Kita13, Nishi8, Kita-ku, Sapporo, Hokkaido, 060-8628 Japan. 3) Lab. Technical Research & Development Bureau NIPPON STEEL & SUMITOMO METAL Corp., 1 Oaza-Nishinosu, Oita City, Oita, 870-0992 Japan. 4) Department of Materials Science and Engineering, Faculty of Engineering, Kyusyu University, 744 Moto-oka, Nishi-ku, Fukuoka, 819-0395 Japan. 5) International Institute for Carbon-Neutral Energy Research (WPI-I2CNER), Kyushu University, 744 Moto-oka, Nishi-ku, Fukuoka, 819-0395 Japan. 6) Interdisciplinary Graduate School of Engineering Sciences, Kyushu University, 6-1 Kasuga-koen, Fukuoka, 816-8580 Japan.

(*Received on May 24, 2016; accepted on July 13, 2016; originally published in Tetsu-to-Hagané, Vol. 102, 2016, No. 5, pp. 253–259*)

To evaluate heterogeneous strain distribution developed by pre-deformations in dual phase (DP) steel accurately, a combinational technique of Electron Backscatter Diffraction (EBSD) and Digital Image Correlation (DIC) methods was newly introduced in this study. A good correlation is established between kernel average misorientation calculated by EBSD and local equivalent strain measured by DIC in ferrite matrix of DP steels regardless of the difference in deformation process, which means that an EBSD orientation map can be easily converted into an applicative strain map by employing the individual correlation formula. This new technique reveals that very large strain region is locally formed within dozens of micrometer from the punched edge in a punched DP steel. On the other hand, hard martensite grains dispersed in DP steel remarkably promote the heterogeneity of strain distribution in ferrite matrix. As a result, the large strain region is also developed in the form of bands in a cold-rolled DP steel by only 60% thickness reduction at least, as if it is affected by the distribution and morphology of martensite grains. In addition, the local strain mapping demonstrates that the equivalent strain of the large strain band in cold-rolled material is comparable to that of the heavily deformed edge in punched one. The very large strain band in ferrite matrix is characterized by ultrafine grained structure, which leads to the possibility for the losing ductility in ferrite matrix and the martensite cracking.

KEY WORDS: local strain mapping; dual phase steel; heterogeneous strain distribution; electron backscatter diffraction; digital image correlation.

1. Introduction

Dual Phase (DP) steel consisting of soft ferrite and hard martensite has been widely used as automotive high strength steel sheet. As well as the further strengthening, good formability, especially stretch flangeability, is strongly required for this kind of steels.[1)] In general, stretch flangeability can be evaluated by hole expansion test, which consists of punching press and hole expansion. It is therefore necessary for development of DP steel with good formability to clarify the changes in microstructure and mechanical properties by severe pre-deformation (punching press) and then to understand how the changes affect the formability on post-deformation (hole expansion). The deformation area formed by punching press is localized within a very narrow region from the punched edge. This limitation of deformation area makes us difficult to investigate the microstructure and mechanical properties. In the previous work, authors tried the investigation using the nano-indentation testing. As a result, it was found that the edge of punched DP steel is significantly strain-hardened by punching press, but the hardness is unexpectedly close to that of cold-rolled one.[2)] This indicates that cold rolling would be appropriate as an

* Corresponding author: E-mail: nakada.n.aa@m.titech.ac.jp
DOI: http://dx.doi.org/10.2355/isijinternational.ISIJINT-2016-310

© 2016 ISIJ

alternate severe pre-deformation process of punching press for investigating the changes in microstructure and mechanical properties of DP steel by severe pre-deformations more easily, because a whole of specimen is uniformly deformed by cold rolling. In order to confirm that, it is more reasonable to absolutely characterize and compare the deformation area in punched DP steel with cold-rolled DP steel not only by nano-hardness testing but also by strain measurement.

Although there are some techniques for strain measurement, the number of techniques having both high accuracy and spatial resolution are limited. As one of them, Electron Back Scatter Diffraction method (EBSD) has become commonplace in materials science. Especially, since the average misorientation between the data point and all of its neighbors, so-called kernel average misorientation (KAM), can be automatically calculated in EBSD (EBSD-KAM), EBSD-KAM is frequently used as a user-friendly method to evaluate strain locally distributed in metallurgical materials.[3] However, it should be noted that the EBSD-KAM is just a crystal rotation angle not strain itself. On the other hand, some of authors recently reported that Digital Image Correlation method (DIC) is able to analyze strain with very high accuracy and spatial resolution, when it is applied to the digital images of metallurgical micrograph, such as scanning electron microscope (SEM) image.[4] Since displacement and strain are optically measured by analyzing the change in digital images between the before and after deformation in DIC, DIC can analyze the strain distributed not in the inside but at the outside of an objective specimen. That is, both EBSD and DIC have merit and demerit, and the strain distributed in the inside of DP steel cannot be analyzed by either of them in principle. However, if we are able to combine only their merits, "to evaluate deformation microstructure developed in the inside of a specimen" in EBSD and "to analysis strain itself" in DIC, the combination technique could enable us to analyze strain distributed in the inside of DP steel accurately.

In order to analyze strain heterogeneously distributed in DP steel accurately, we provided a new combinational technique of EBSD and DIC in this study. First, the correlation between EBSD-KAM and equivalent strain measured by DIC was verified. And then, feature of strain distribution in punched material was compared with that in cold-rolled one using the new combination technique based on the individual correlation between them.

2. Experimental Procedure

Two steels with different carbon content were used in this study, whose chemical compositions are listed in **Table 1**. These steels were austenitized at 1 373 K for 600 s, and then isothermally held at 983 K in ferrite and austenite two phase region for 1.8 ks, followed by water-quenching to promote a martensitic transformation of untransformed austenite. After the heat treatment, these steels had DP structure consisting of ferrite and martensite with different fraction. The microstructure was observed by optical and scanning electron microscopy. EBSD was conducted using field emission scanning electron microscopes with EBSD system (FE-SEM/EBSD: Ultra 55 developed by Carl Zeiss and JSM-7001F developed by JEOL Ltd.). Working distance and step size for EBSD were set as 15 mm and 0.5 μm, respectively. The captured EBSD patterns were analyzed by a software, OIM analysis ver 7.1.0 developed by TSL solutions. EBSD-KAM was determined by first nearest-neighbor points in hexagonal grid under a condition that the misorientation angle greater than 5° is ignored. As for DIC, the microstructure clearly developed by the deep etching with 3% nital and 10% sodium hyposulfite solution was captured as digital image before and after a deformation at the same position using SEM (VE-9800 developed by Keyence). These images were applied to a DIC software, VIC-2D developed by Correlation Solutions, to analyze the amount and distribution of strains quantitatively.[4] In this study, the amount of strain was evaluated as equivalent strain. Subset size and step size for DIC were set to be 41×41 pixels and 5 pixels, respectively. The resolution of a SEM image was controlled in order for the step size in DIC (5 pixels) to be same as that in EBSD (0.5 μm). The same view field observation for EBSD and DIC was carried out on a flat plane of tensile deformed specimens and a side plane of cold-rolled specimens. Tensile testing was conducted at an initial strain rate of 1.67×10^{-3} s^{-1} for plate test pieces with a gauge size of $6^{l}\times3^{w}\times1^{t}$ mm^3. In addition, a deformation microstructure of ferrite matrix was characterized using a transmission electron microscope (TEM, JEM-2000FX developed by JEOL). TEM samples with volume of $30^{l}\times10^{w}\times5^{t}$ μm^3 were sampled from ferrite matrix in the vicinity of a martensite grain and then thinned to less than 100^{t} nm by Focused Ion Beam systems (FIB, Versa 3D developed by FEI and JEM-9320FIB developed by JEOL). Macroscopic equivalent strain by cold rolling ε_{eq} was calculated under von Mises' condition, as follows.

$$\varepsilon_{eq} = -\frac{2}{\sqrt{3}} ln \frac{t}{t_0} \quad \text{..... (1)}$$

Here, t_0 and t are thickness of specimens before and after cold rolling. Punching press was carried out for plate test pieces of 80×80×0.6 mm^3 using a die having a hole with diameter of 10 mm at 12.5% clearance.

Table 1. Chemical compositions of DP steels used in this study (mass%).

	C	Si	Mn	P	S	Al	N	Fe
M10	0.049	0.005	1.01	<0.002	0.0007	0.016	0.0013	Bal.
M30	0.14	0.005	1.00	<0.002	0.0007	0.015	0.0012	Bal.

3. Results and Discussion

3.1. Correlation between DIC Strain and EBSD-KAM

The optical micrographs of DP steel with different martensite fraction are represented in **Fig. 1**. They have a typical DP structure consisting of ferrite matrix with average grain size of 60 μm and blocky martensite grains. Although the martensite fraction is different between (a) 12% and (b) 19%, they have almost the same hardness, (a) 6.12 GPa and (b) 5.90 GPa. In the following, according to its martensite fraction, they are named as (a) M10 and (b) M30, respectively.

Figure 2 shows an example of the same view field obser-

© 2016 ISIJ

vation of DIC and EBSD in 5% tensile-deformed M10. Images (a) and (b) show DIC equivalent strain map overlaid on the corresponding SEM image and bcc inverse pole

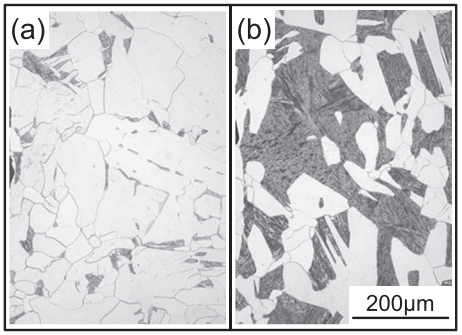

Fig. 1. Optical micrographs of dual phase steel with different martensite fraction. (a) M10, (b) M30.

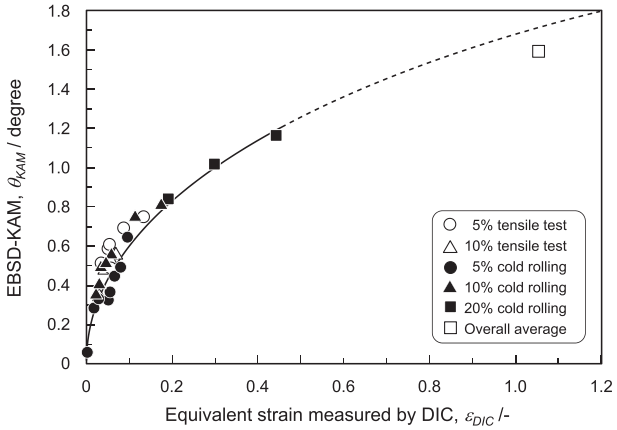

Fig. 3. Relation between strain measured by DIC and EBSD-KAM value in ferrite matrix of tensile deformed and cold-rolled M10 DP steel.

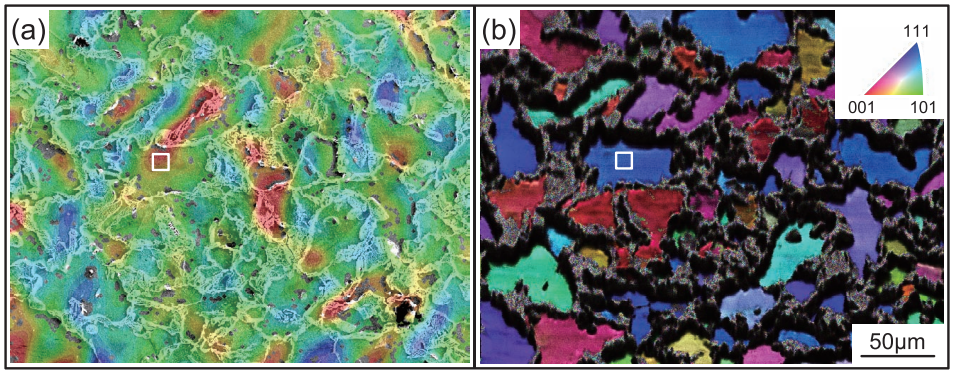

Fig. 2. Strain map laid on SEM image (a) and inverse pole figure map (b) of M10 DP steel taken at the same position.

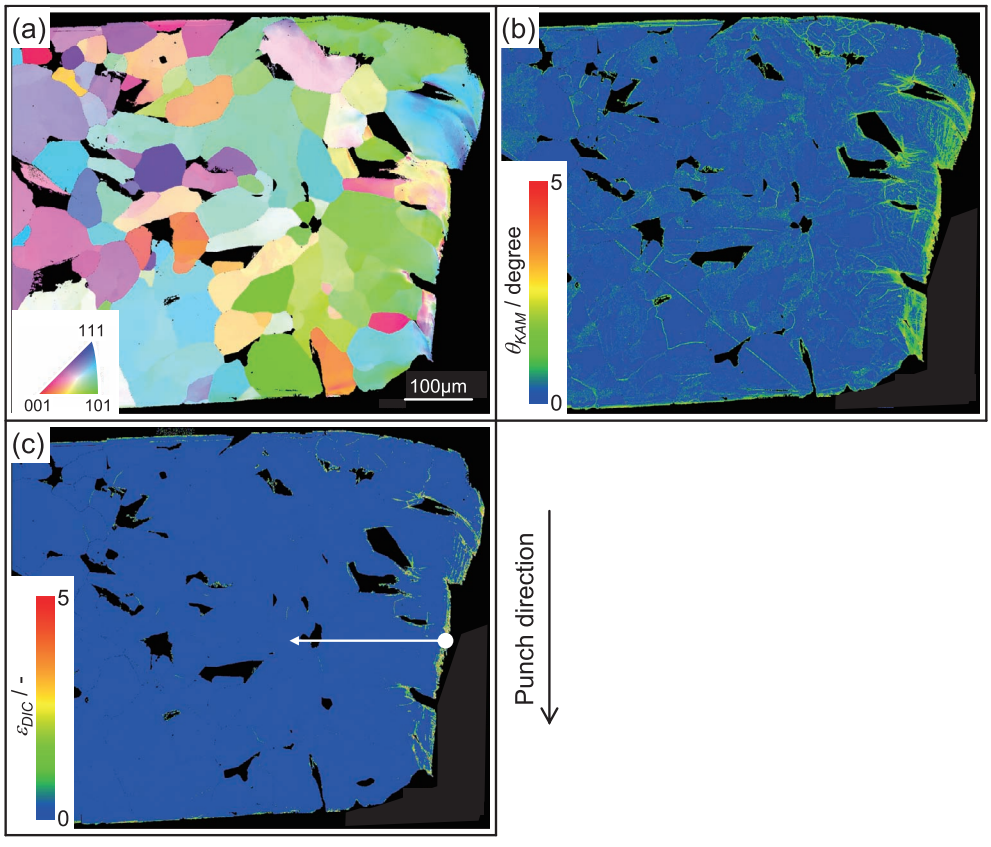

Fig. 4. Inverse pole figure (a), EBSD-KAM (b) and strain (c) maps of ferrite matrix in punched M10 DP steel.

© 2016 ISIJ

figure (bcc-IPF) map with image quality (IQ) evaluated by EBSD, respectively. It is found in map (a) that local strain distribution can be analyzed even in ferrite matrix by deep etching, although the ferrite has no substructure. However, since the deep etching roughed grain boundaries and substructure of martensite grains, these areas were cannot be analyzed by EBSD. As a result, measureable data in EBSD were limited only in the inside of each ferrite grain (b). This demonstrates that both of strain and crystal orientation are simultaneously analyzed at the same position of ferrite grains in DP steel. Equivalent strain calculated by DIC; ε_{DIC} and EBSD-KAM; θ_{KAM} that were obtained from the same position are plotted in **Fig. 3**. In this analysis, ε_{DIC} and θ_{KAM} were averaged within an area of 8×8 μm^2, as indicated by a white square in Fig. 2[†1]. When an applied strain in tensile testing and a reduction thickness in cold-rolling were greater than 10% and 20% (ε_{eq} = 0.26), respectively, the observation area at a specimen surface became so wavy that DIC could not be performed. But, fortunately, heavily deformed areas with 0.4 in ε_{DIC} was locally developed in 20% cold rolling material, which enables to verify the relationship between ε_{DIC} and θ_{KAM} in a relatively wide range. Plastic deformation causes crystal rotation in metal, thus θ_{KAM} should increase monotonically with increasing ε_{DIC}. The common trend is identified in this figure and the correlation between ε_{DIC} and θ_{KAM} can be formulated by the following power law.

$$\theta_{KAM} = \frac{\pi}{180} 1.68 \varepsilon_{DIC}^{0.44} \quad \text{(rad)} \quad \cdots\cdots\cdots\cdots (2)$$

The fact that the determination coefficient of this formula R^2 is high than 0.9 proves that a good correlation is established between ε_{DIC} and θ_{KAM} in ferrite matrix of DP steels. In addition, the both data of tensile-deformed and cold-rolled materials are plotted with an identical curve, which may reveal that this correlation formula is independent of the deformation process. A very large ε_{DIC} cannot be achieved experimentally due to losing a smoothness of specimen surface, as mentioned above. However, it is found that this relationship is realized even in 60% cold-rolled M10 as indicated by the open square when the average EBAD-KAM that is obtained from a wide area on the cross section of specimen is plotted with macroscopic equivalent strain of whole specimen (ε_{eq}=1.06). This implies that this correlation formula may be established even in larger strain region. Here, we should notice that this formula has no physical meaning and can be used only in this study. Because, ε_{DIC} and θ_{KAM} are thought to depend on crystal structure, chemical composition of objective metal and deformation temperature, as well as the measurement conditions of EBSD and DIC.

3.2. Local Strain Distribution in Punched DP Steel

Cross sectional image of punched M10 is shown in **Fig. 4**. Maps (a) and (b) are bcc-IPF map expect for martensite grains and the corresponding EBSD-KAM map, respectively. In addition to them, map (c) is the local strain map converted from (b) by employing Eq. (2). The punched edge has a fracture surface characterized by shear and fracture planes and ferrite matrix was plastically deformed accompanied with a significant crystal rotation (a). In response to this, map (b) shows that EBSD-KAM becomes higher gradually as coming closer to the punched edge and the area with high EBSD-KAM expands to a depth of approximately 100 μm. Even though map (c) has the same tendency as map (b), it proves that the region with large strain is localized in the vicinity of the punched edge and the width is very narrow. The difference between them is attributed from the fact that the relation between local strain and EBSD-KAM is formulated by power law. This provides attention that small strain region is greatly exaggerated when EBSD-KAM is regarded as an indication of strain in a conventional manner. The strain profile across a martensite grain from the punched edge to the interior of specimen along the white line in map (c) is shown in **Fig. 5**. Very large strain region is locally formed within approximately 20 μm from the punched edge in a punched DP steel, whose average equivalent strain is 2.0 and maximum one is 4.0. In the previous research,[5] the finite element method analysis revealed that the equivalent strain at the punched edge reaches about 3.0. Comparing with the analytical result, it is thought that the quantitative performance of this new strain measurement is yet insufficient, however, the prospection isn't bad even in large strain level. In either case, it is a fact that very large strain region is locally formed within dozens of micrometer from the punched edge and should have a large influence on the formability upon the subsequent hole expansion in a punched DP steel. In addition, it is worth noting in Fig. 5 that the strain distribution is heterogeneous depending on the DP structure. Strain is negligible within ferrite grains sufficiently distant from the punched edge, while a certain

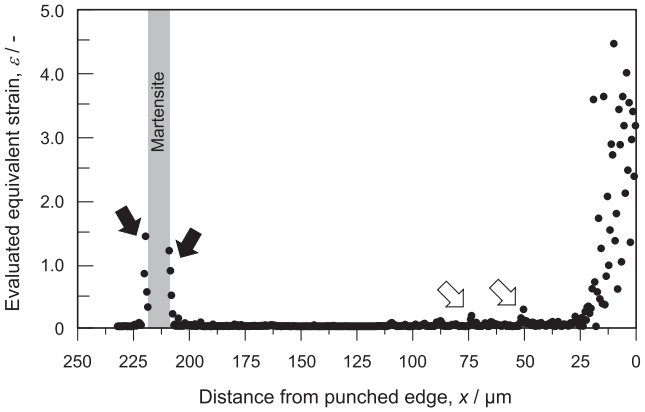

Fig. 5. Equivalent strain profile in ferrite matrix on cross-section at the punched M10 DP steel. Strain was measured along the white line in Fig. 3(c).

[†1]: The similar correlation is confirmed between ε_{DIC} and θ_{KAM} even when the averaging area becomes large. On the other hand, it is too hard to make the positions for DIC and EBSD match each other as the averaging area becomes much small. Therefore, the area was determined as the smallest area to measure the local strain distribution by trial and error.

[†2]: Since the maximum value of EBSD-KAM was set at 5° in this analysis, θ_{KAM} must be close to 5° as ε_{DIC} is infinite. Therefore, the correlation between ε_{DIC} and θ_{KAM} should not be formulated by a power law. However, θ_{KAM} reaches to 5° when ε_{DIC} is larger than 12 in the formula. This means that Eq. (2) is useful within the strain region discussed in this study.

© 2016 ISIJ

strain is accumulated at ferrite grain boundaries (white arrows) and ferrite/martensite interfaces (black arrows). In particular, the fact that the strain is larger than 1.0 at ferrite/martensite interface that is 200 μm or more apart from the punched edge demonstrates that hard martensite grains dispersed in DP steel remarkably promote the heterogeneity of strain distribution in ferrite matrix.

3.3. Local Strain Distribution in Cold-rolled DP Steel

Cross sectional image of 60% cold-rolled M10 observed from normal direction (ND) is represented in **Fig. 6**. Maps (a) and (b) are ND-IPF map of ferrite matrix before and after cold rolling, respectively. Map (c) is EBSD-KAM map calculated from (b), and furthermore, map (d) is the local strain map converted from (b). Crystal orientation of ferrite was significantly changed by cold rolling (a → b). Although EBSD-KAM map (c) gives misleading information showing that strains seems to be accumulated uniformly in a whole of specimen, local strain map (d) clearly demonstrates that strains are heterogeneously distributed in ferrite matrix in cold-rolled DP material. Especially, it is found that in map (d) that large strains colored by green and yellow are located not only at ferrite/martensite interfaces but also within ferrite matrix in the form of bands perpendicularly to rolling direction (RD). The large strain bands (LSB) seem to be developed while connecting martensite grains. The strain profile across a martensite grain along the white line in map (d) is shown in **Fig. 7**. The profile of strains at ferrite/martensite interface (black arrows) is higher and wider compared with that in punched material (see in Fig. 5) due to the macroscopically uniform deformation of specimen by cold rolling. In addition, LSB pointed by white arrows has the similar large strain profile. The histogram of local strain in Fig. 6(d) were displayed in **Fig. 8** so as to evaluate the heterogeneity of strain distribution. The arithmetical mean

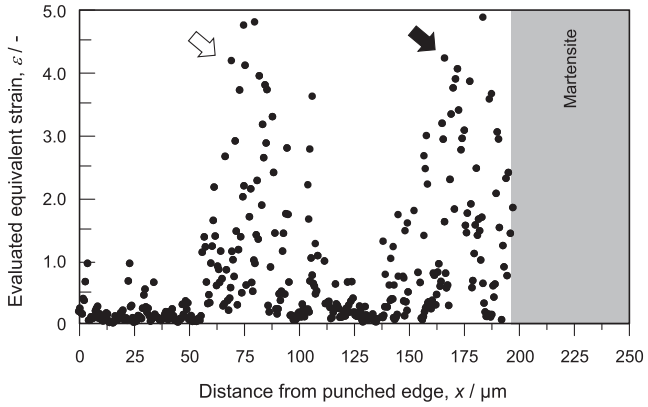

Fig. 7. Equivalent strain profile in ferrite matrix of 60% cold-rolled M10 DP steel. Strain was measured along the white line in Fig. 6(d).

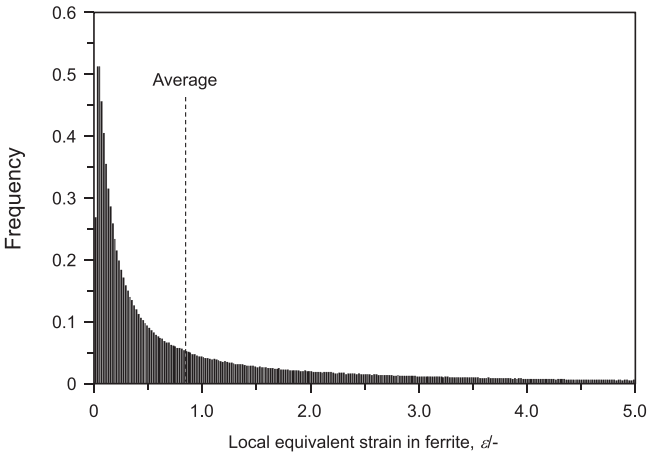

Fig. 8. Local strain distribution profile in ferrite matrix of 60% cold-rolled M10 DP steel.

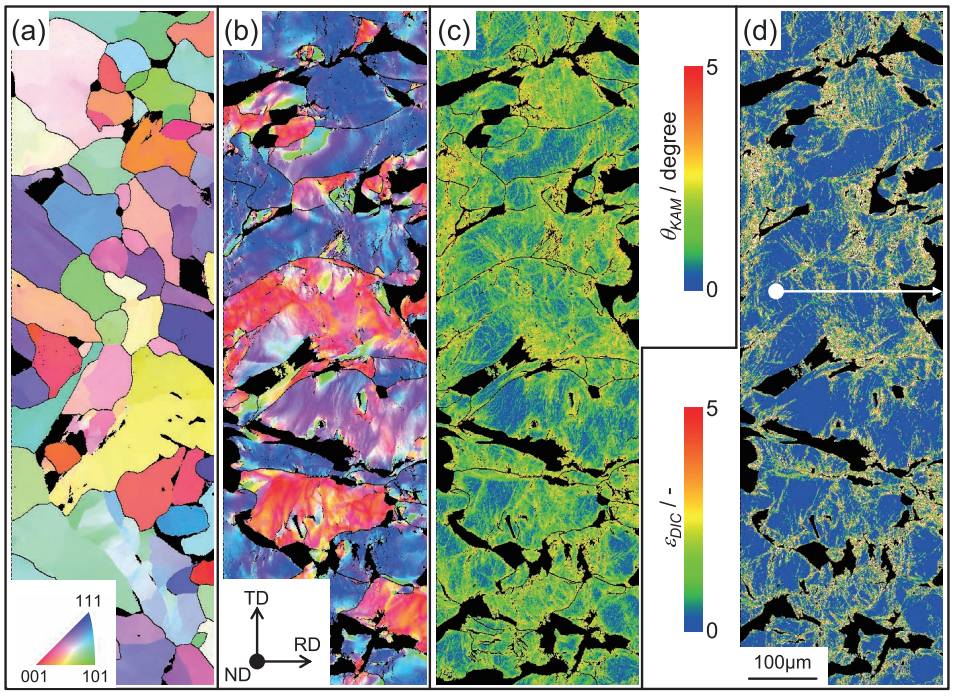

Fig. 6. Initial (a) and 60% cold-rolled (b–d) M10 DP steels. (a, b) inverse pole figure map, (c) EBSD-KAM map and (d) strain map.

© 2016 ISIJ

and the standard deviation of this histogram are measured to be 0.85 and 1.04, respectively. These value is much greater than the most frequent strain value, approximately 0.04, which suggests that most areas of ferrite matrix are hardly deformed, while LSB observed in Figs. 6(d) and 7 frequently forms even after 60% cold rolling. In fact, the fraction of large strain areas with higher than 2.0 in local strain is counted at 14% in the histogram. Judging from the amount of measured strain, it is thought that LSB has the deformation microstructure similar to heavily deformed area at the edge of punched DP material as shown in Figs. 4 and 5. In order to investigate the microstructure of LSB in detail, M30 with larger martensite fraction was used for the following microstructural characterizations.

Figure 9 shows ND cross-sectional SEM image of 60% cold-rolled M30. This image was taken by a special detector which can detect low-angle backscattered electron signals selectively (Angle Selective Backscattered Electron Detector), thus substructures in a martensite grain and deformation microstructures in ferrite matrix can be clearly observed due to an electron channeling contrast effect. The SEM image indicates that a couple of cracks form in a martensite grain perpendicularly to RD. The left crack passes through the martensite grain, while the right one stays in that.

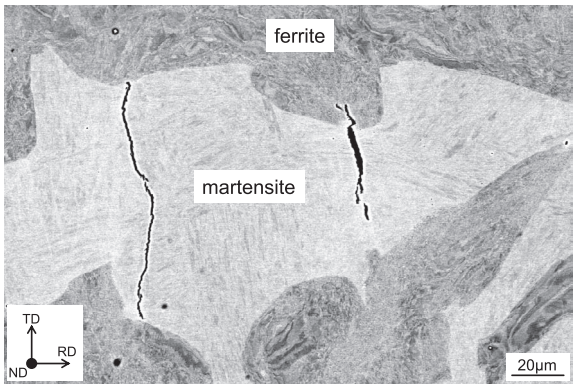

Fig. 9. Angle Selected Backscatter SEM image showing a couple of cracks growing within a martensite grain in 60% cold-rolled M30 DP steel.

Especially, the right crack seems to be propagating across a necked part of the martensite grain. EBSD data obtained at the same positon are represented in **Fig. 10**. Maps (a), (b) and (c) correspond to IQ, bcc-IPF and local strain maps, respectively. In these maps, the cracks in martensite are drawn by while dotted lines and the edges were pointed by white arrows. Maps (a) and (b) reveal that ferrite matrix is largely plastic-deformed, while the martensite grain maintains transformation substructures. This demonstrates that martensite grains hardly deformed in DP structure, however, it was confirmed in the previous study using DIC that such blocky martensite grains is slightly plastic-deformed.[6] Crystallographic analysis says that all martensite blocks in the martensite grain with cracks have an identical crystal orientation characterized as Kurdjumov-Sachs orientation relationship,[7] which demonstrates that this martensite grain had transformed from a prior austenite grain. When we look at the relation between the martensite substructures and the propagating cracks, it is found that the cracks pass through some specific boundaries, *i.e.* packet and block boundaries, meaning that the martensite cracking is caused not at brittle fracture mode but at ductile one. Comparing the position of martensite cracks with the distribution of LSB in ferrite matrix in map (c), LSB tend to be at the front of the crack-tips. This result emphasizes that the martensite cracking connections with the formation of LSB and there are two possible mechanisms; (1) ductile fracture takes place in hard martensite grain preferentially by cold rolling and then the ductile crack propagates toward ferrite matrix accompanied with the formation of LSB. On the other hand, (2) LSB forms in ferrite matrix preferentially, leading to the ductile cracking in martensite grains due to stress concentration. It should be noted here that LSB distributes widely at the front of the right-bottom crack-tip, even though it has not reached the ferrite/martensite interface, as indicated by A in map (c). Furthermore, it is generally thought that a plastic zone at crack-tip is small, but LSB develops as long as the length of crack (50–100 μm). From these results, it can be concluded that the martensite cracking is induced by the formation of LSB. Considering that the crack propagates

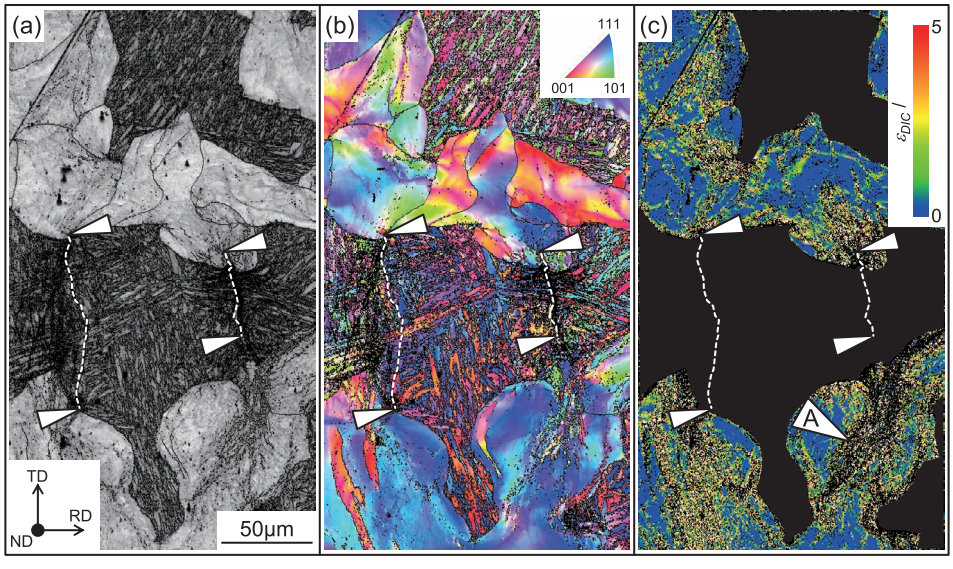

Fig. 10. IQ (a), inverse pole figure (b) and strain (c) maps of ferrite matrix in punched M30 DP steel.

© 2016 ISIJ

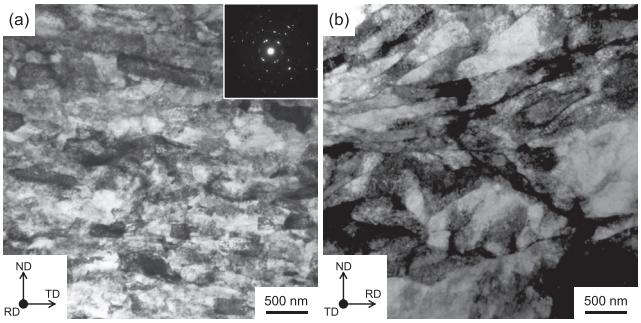

Fig. 11. BF-TEM images of RD plane (a) and TD plane (b) in 88% cold-rolled M30 DP steel.

along the necked part of martensite grain, LSB is thought to be developed depending on a distribution and a morphology of martensite grains. When such pre-deformed DP steel is further deformed, ductile crack in martensite should propagate along LSB in ferrite matrix, leading to the fracture of a material. Therefore, it is necessary to investigate the feature of microstructure and mechanical properties, especially ductility, of LSB. Microstructure of LSB is mentioned in the following part, while mechanical properties will be reported in the continued report.[8] **Figure 11** is (a) RD and (b) TD cross-sectional TEM bright field images showing ferrite matrix in the vicinity of a martensite grain in 88% cold-rolled M30. It was prospectively validated before FIB sampling using EBSD data that the observation area corresponds to LSB as seen in Figs. 6 and 7. The ferrite matrix has elongated ultrafine grain structure with high density dislocations, whose grain size was measured at 400 nm in width and 200 nm in thickness. In addition, since the diffraction pattern obtained from the observation area shows multiple diffraction spots with a streak, it is found that each ferrite grain is surrounded by high-angle grain boundaries. From this characterization, the microstructure of LSB is identified to be similar to the ultrafine-grained structure formed at the edge of punched DP steel.[9] Considering that the thickness of ferrite grain along ND is calculated to be around 10 μm after cold rolling from the initial ferrite grain size, it is concluded that such ultrafine-grained structure forms via dynamic grain refinement. According to the previous researches on the formation of ultrafine-grained structure by sever plastic deformation, such elongated ultrafine grain structure is developed by large strain from 4 to 5 in equivalent strain.[10] The large strain is substantially coincident with the strain in LSB evaluated by local strain mapping. From these results, LSB developed in cold-rolled DP material agrees with the heavily deformed structure formed by punching press and is identified as ultrafine-grained structure or its precursive deformation structure formed by sever plastic deformation. Based on these results, mechanical properties of ferrite, martensite and ferrite/martensite interface in cold-rolled DP steel will be individually evaluated by micro tensile testing in the continued report.

4. Conclusions

To evaluate heterogeneous strain distribution developed by pre-deformations in dual phase (DP) steel accurately, a combinational technique of Electron Backscatter Diffraction (EBSD) and Digital Image Correlation (DIC) methods was newly introduced. And then, the feature of strain distributed in ferrite matrix was compared between punched and cold-rolled DP steels using the combination technique. The obtained results are as follows.

(1) A good correlation is established between kernel average misorientation calculated by EBSD and local equivalent strain measured by DIC in ferrite matrix of DP steels regardless of the difference in deformation process. By employing the individual correlation formula, EBSD orientation map can be easily converted into an applicative strain map that is able to visualize the strain distribution with both high accuracy and spatial resolution.

(2) In punched DP steel, very large strain region with higher than 2.0 in average equivalent strain is formed within dozens of micrometer from the punched edge. Meanwhile, hard martensite grains dispersed in DP steel remarkably promote the heterogeneity of strain distribution even within ferrite grains sufficiently distant from the punched edge.

(3) In cold-rolled DP steel, large strain band is formed within ferrite matrix depending on the distribution and morphology of martensite grains. The formation and development of large strain band leads to a ductile fracture of martensite grains.

(4) The large strain band formed in cold-rolled DP steel has ultrafine-grained structure or its precursive deformation structure formed by sever plastic deformation. Judging from the amount of equivalent strain measured by local strain mapping and the characteristics of microstructure, the large strain band is identified to be same as the very large strain region formed at the edge of punched DP steel.

Acknowledgment

This study was supported by a Grant-in-Aid for Scientific Research (C) No. 15K06488 (2015–2018) from the Japan Society for the Promotion of Science and 23th ISIJ Research Promotion Grant.

REFERENCES

1) M. Takahashi, H. Kohno, T. Hayashida, R. Okamoto and Y. Taniguchi: *Shinnittetsu Giho*, **378** (2003), 7.
2) H. Shuto, T. Ohmura, T. Yokoi and A. Uenishi: *CAMP-ISIJ*, **27** (2014), 495.
3) M. Calcagnotto, Y. Adachi, D. Ponge and D. Raabe: *Acta Mater.*, **59** (2011), 658.
4) N. Nakada, M. Nishiyama, N. Koga, T. Tsuchiyama and S. Takaki: *Tetsu-to-Hagané*, **100** (2014), 1238.
5) T. Matsuno, Y. Kuriyama, S. Yonezawa, H. Murakami and N. Ohtake: *J. Jpn. Soc. Technol. Plast.*, **53** (2012), 836.
6) K. S. Park, M. Nishiyama, N. Nakada, T. Tsuchiyama and S. Takaki: *Mater. Sci. Eng. A*, **604** (2014), 135.
7) S. Morito, H. Tanaka, R. Konishi, T. Furuhara and T. Maki: *Acta Mater.*, **51** (2003), 1789.
8) S. Ogata, Y. Mine, K. Takashima, T. Ohmura, H. Shuto and T. Yokoi: *ISIJ Int.*, **56** (2016), 2084.
9) T. Yokoi, H. Shuto, K. Ikeda, N. Nakada, T. Tsuchiyama, T. Ohmura, Y. Mine and K. Takashima: *ISIJ Int.*, **56** (2016), 2068.
10) T. Maki, T. Furuhara, N. Tsuji, S. Morito, G. Miyamoto and A. Shibata: *Tetsu-to-Hagané*, **100** (2014), 1062.

© 2016 ISIJ